Fuel 325 (2022) 124764

Contents lists available at ScienceDirect

Fuel

journal homepage: www.elsevier.com/locate/fuel

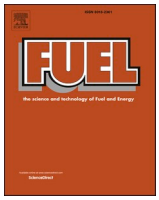

Full Length Article

Aircraft engine particulate matter emissions from sustainable aviation fuels: Results from ground-based measurements during the NASA/DLR campaign ECLIF2/ND-MAX

Tobias Schripp [a,*], Bruce E. Anderson [b], Uwe Bauder [a], Bastian Rauch [a], Joel C. Corbin [c], Greg J. Smallwood [c], Prem Lobo [c,1], Ewan C. Crosbie [b], Michael A. Shook [b], Richard C. Miake-Lye [d], Zhenhong Yu [d], Andrew Freedman [d], Philip D. Whitefield [e], Claire E. Robinson [b], Steven L. Achterberg [e], Markus Köhler [a], Patrick Oßwald [a], Tobias Grein [a], Daniel Sauer [f], Christiane Voigt [f,g], Hans Schlager [f], Patrick LeClercq [a]

[a] German Aerospace Center (DLR), Institute of Combustion Technology, Stuttgart, Germany
[b] NASA Langley Research Center, Hampton, VA, USA
[c] Metrology Research Centre, National Research Council Canada, Ottawa, ON, Canada
[d] Aerodyne Research Inc., Billerica, MA, USA
[e] Center of Excellence for Aerospace Particulate Emissions Reduction Research, Missouri University of Science and Technology, Rolla, MO, USA
[f] German Aerospace Center (DLR), Institute of Atmospheric Physics, Oberpfaffenhofen, Germany
[g] Institute of Atmospheric Physics, University Mainz, Mainz, Germany

ARTICLE INFO

Keywords:
HEFA
SAF
Ultra-fine particles
Sustainability

ABSTRACT

The use of alternative jet fuels by commercial aviation has increased substantially in recent years. Beside the reduction of carbon dioxide emission, the use of sustainable aviation fuels (SAF) may have a positive impact on the reduction of particulate emissions. This study summarizes the results from a ground-based measurement activity conducted in January 2018 as part of the ECLIF2/ND-MAX campaign in Ramstein, Germany. Two fossil reference kerosenes and three different blends with the renewable fuel component HEFA-SPK (Hydroprocessed Esters and Fatty Acids Synthetic Paraffinic Kerosene) were burned in an A320 with V2527-A5 engines to investigate the effect of fuel naphthalene/aromatic content and the corresponding fuel hydrogen content on non-volatile particle number and mass emissions. Reductions up to 70% in non-volatile particle mass emission compared to the fossil reference fuel were observed at low power settings. The reduction trends to decrease with increasing power settings. The fuels showed a decrease in particle emission with increasing fuel hydrogen content. Consequently, a second fossil fuel with similar hydrogen content as one of the HEFA blends featured similar reduction factors in particle mass and number. Changes in the fuel naphthalene content had significant impact on the particle number emission. A comparison to in-flight emission data shows similar trends at cruise altitudes. The measurements highlight the importance of individual fuel components in regulating engine emissions, particularly at the low thrust settings typically employed during ground operations (e.g. during idle and taxi). Therefore, when selecting and mixing SAF blends to meet present fuel-certification standards, attention should be paid to minimizing complex aromatic content to achieve the greatest possible air quality and climate benefits.

1. Introduction

In 2019, the global aviation fuel demand reached approx. 331 Mt (9.7 G gallons (U.S.)) [1] and showed an average annual growth rate of approx. 3% over the past 30 years. In 2020, the impacts of the COVID19 pandemic on air traffic led to a reduced fuel demand. According to the

* Corresponding author.
E-mail address: tobias.schripp@dlr.de (T. Schripp).
[1] Current affiliation: Office of Environment and Energy, Federal Aviation Administration, Washington, D.C. 20591, USA.

https://doi.org/10.1016/j.fuel.2022.124764
Received 14 February 2022; Received in revised form 17 May 2022; Accepted 2 June 2022
Available online 24 June 2022

United States Energy Information Administration (EIA), the jet fuel consumption from commercial passenger aircraft dropped to 20% of the previous year's demand in April/May 2020, but has largely recovered since then [2]. The reduced air traffic led to changes in the atmospheric composition at cruise altitudes [3,4], and in a reduced contrail cover and climate impact [5,6]. Even though the pandemic caused a significant reduction in fuel demand for certain periods, the aviation sector will continue to require large quantities of cost-efficient kerosene in the near future. Beside labor costs, fuel costs are the second most important cost factor in aviation. The volatility of the jet fuel price coupled with the need to use sustainable forms of energy calls for "drop-in" alternatives. However, current production of sustainable aviation fuels (SAF) is miniscule compared to the actual demand, and price point is also a consideration that affects further growth in production. According to the International Air Transport Association (IATA), 100 M litres (26.4 M gallons (U.S.)) of SAF will be produced in 2021 [7]. Based on the current values, the production of SAF will lag behind the demand for many years to come and, thus, the available fuel quantity must be used as efficiently as possible to achieve a reduction of particle emissions and associated contrail formation [8,9]. This "smart" usage of alternative jet fuels includes the optimal selection of the blending components to obtain the lowest possible environmental impact.

One of the most prominent commercially available SAF components is HEFA-SPK (Hydroprocessed Esters and Fatty Acids Synthetic Paraffinic Kerosene). Currently, ASTM D7566 allows up to a maximum of 50% HEFA by volume to be blended with fossil Jet A or Jet A-1. Technically, lower blending ratios might be necessary to comply with the ASTM restrictions for density, freezing point and minimum aromatic content. Due to the compositional complexity of the fuel mixture, the prediction of physical properties needs sophisticated methods in lieu of measurements [10]. HEFA is free of aromatic species, which may impact seal swell in older jet engines [11] and currently limits routine use of pure HEFA. Nevertheless, emission studies with aromatic-free jet fuels have been performed on a CFM56-7B engine [12], a CFM56-2C1 [13] and a CFM56-5C4 engine [14] without any reported engine-related problems. Boeing recently announced a commitment to ensure that all its commercial airplanes can fly on and gain certification to use 100% sustainable aviation fuels by 2030 [15] and indeed the first commercial flight with passengers on board has been performed successfully [16]. The future use of pure SAF appears promising with additional benefits that come with the lack of aromatic species and sulfur compounds. Both aspects are advantageous with regard to the formation of contrails [17–19] even though the soot formation mechanism of contrails dominates for soot emission indices above 1–2 * 10^{14} #/kg fuel [20].

Several scientific studies focused on the non-CO_2 emissions of aircraft jet engines in particular. Alternative jet fuels and blends with higher fuel hydrogen content than regular jet fuel produce less soot during combustion, which has been proven in many field studies [8,14,21–26]. The application of ternary blends with beneficial emission properties has been demonstrated on PW4158 engines as well [27]. It must be noted that the reduction in emission is a function of the jet engine power setting, with the largest reductions usually observed at idle and low power conditions. Elser et al. [25] analyzed emissions from a CFM56-7B engine burning different blends of Jet A-1 and HEFA. For the highest HEFA blend (32%) they observed a reduced emission of elemental carbon (EC) mass in the range of 50% − 60% at low power settings. Moore et al. [28] observed >90% nvPM mass- and number-emission reductions when burning pure SAF in a CFM56-2C1 engine

Table 1
Selected physico-chemical parameters of the fuels used.

Fuel	Ref3	Ref4	SAJF1	SAJF2	SAJF3
Components	Jet A-1	Jet A-1	51 vol% Ref3 + 49 vol% HEFA-SPK	70 vol% Ref4 + 30 vol% HEFA-SPK	49 vol% Ref3 + 34 vol% Ref4 + 17 vol% HEFA-SPK
Aromatics [%v/v] (ASTM D1319)	18.6	16.5	8.5	9.5	15.2
Density (15 °C) [kg/m^3] (ASTM D4052)	814.4	790.5	784.4	777.3	761.1
Viscosity (-20 °C) [mm^2/s] (ASTM D445)	4.591	3.251	4.332	3.244	3.961
Specific energy [MJ/kg] (ASTM D3338)	43.138	43.340	43.629	43.632	43.358
Smoke point [mm] (ASTM D1322)	23.0	27.0	30.0	30.0	28.0
Naphthalene content [%v/v] (ASTM D1840)	1.17	0.13	0.61	0.05	0.64
Sulfur, total [%m/m] (ASTM D2622)	0.012	<0.001	0.007	<0.001	0.007
Sulfur, total [mg/kg] (DIN EN ISO 20884)	105	5.7	56.8	< 5	58.6
Hydrogen content [%m/m] (ASTM D7171)	13.65	14.08	14.40	14.51	14.04
Distillation curve (ASTM D86)					
Initial boiling point [°C]	152.2	149.9	148.8	147.8	150.7
10 vol% recovered [°C]	180.2	163.0	171.1	161.4	170.2
50 vol% recovered [°C]	203.8	186.6	204.1	186.2	196.5
90 vol% recovered [°C]	244.7	220.2	246.4	230.2	239.3
Final boiling point [°C]	271.2	236.1	264.5	247.4	266.5
GCxGC*					
n-paraffins [%m/m]	15.3	22.1	16.8	22.4	18.3
iso-paraffins [%m/m]	20.1	24.1	48.8	40.1	31.0
monocyclic paraffins [%m/m]	28.5	27.9	14.9	20.3	24.0
bicyclic paraffins [%m/m]	13.5	7.5	7.3	4.4	9.2
polycyclic paraffins [%m/m]	0.7	0.1	0.3	0.1	0.4
n-, *iso*-alkylbenzenes [%m/m]	12.3	14.2	6.7	9.9	10.6
cyclo-alkylbenzenes [%m/m]	7.6	3.9	4.1	2.7	5.4
bicyclic aromatics [%m/m]	2.0	0.2	1.1	0.1	1.1

* provided by Sasol.

at low thrust settings and >60% reductions from 50% blends under the same operating conditions. Schripp et al. [14] showed a reduction of 70% particle mass using pure alcohol-to-jet (ATJ) fuel on a CFM56-5C4 engine at the lowest power setting tested. Similar reductions were observed in chase-flight studies using HEFA blends on CFM56-2-C1 engines [8].

Significant reductions in aircraft-engine particulate matter (PM) number emissions are necessary to reduce the climate impact of soot-induced contrails [29]. Recent studies show that when compared with standard petroleum fuels, the lower soot or non-volatile PM (nvPM) emissions associated with burning blended SAFs reduce contrail ice particle number concentrations and lifetimes and thus partially mitigate climate impacts [30]. Overall, soot emission levels and microphysical properties are altered by the changes in fuel composition, particularly by the types and fractions of aromatic species. The lower aromatic-content alternative jet fuels not only produce fewer nvPM emissions, but the particles are smaller [8,23,31] with different morphologies as determined by electron microscopy [32,33], which might also lessen their ice-forming ability. Recently, detailed experimental and modeling studies on the chemical reaction kinetics of complex technical fuels [34–36], have become available and include the fuels investigated herein. These studies highlight the influence of the naphthalene content to the PAH and soot precursor chemistry [36,37] even beyond established correlations such as the hydrogen content. Nevertheless, the emissions from jet engines are affected by numerous influence parameters under real operational conditions. Therefore, the mitigation potential of SAF for non-CO_2-emissions has to be demonstrated in field experiments. The observation and quantification of the emission reduction using SAF at cruising altitudes is, however, associated with an enormous experimental effort, which further limits the amount of available field data and has motivated the combined ground and airborne campaign described in this and companion papers [9,38–40].

This paper presents the results of the ground-based measurement campaign performed during the joint NASA/DLR Multidisciplinary Airborne Experiment (ND-MAX), which examined the effects of fuel composition on aerosol and trace-gas emissions and contrail properties produced by the DLR Advanced Technology Research Aircraft (ATRA) during both ground and airborne operations [9]. ND-MAX incorporated the objectives and work-plan of the second campaign of the Emission and Climate Impact of Alternative Fuel (ECLIF2) project of the German Aerospace Center (DLR). The first ECLIF campaign demonstrated the impact of jet fuels with different hydrogen contents at ground level [23] and inflight [30]. ECLIF2 involved ground test runs with three SAF blends and two reference fuels on an IAE V2527-A5 jet engine. The goal of the ground-based measurements was to investigate the impact of fuel composition on PM emissions produced by the V2527-A5 engine. In addition, the campaign aimed to demonstrate the efficient ("smart") usage of the HEFA blending component to achieve low-emission performance.

2. Materials and methods

The ECLIF2/ND-MAX campaign was performed in January 2018 at the US Air Base in Ramstein, Germany. Ambient temperature conditions during the ground test measurements ranged between 2.3 °C and 8.3 °C (median 2.9 °C). The relative humidity was very high (95 ± 5)%. During the experiment, the main wind direction was from the east (Fig. SI1). Five different fuels were tested during the campaign (Table 1). Two fossil reference Jet A-1 fuels were purchased from different refineries and transported to Ramstein. The abbreviations Ref3 and Ref4 are used to avoid confusion with Jet A-1 fuels used during previous activities in the ECLIF campaign [23]. The three sustainable alternative jet fuel blends (SAJF1-3) were mixtures of the reference fuels and HEFA-SPK. The HEFA component was produced at the World Energy Oil Refinery in Paramount California and purchased from Air bp Hamburg, Germany. The fuels and fuel blends used in this study met the ASTM D1655 [41] certification standard for Jet A-1. The main fuel strategy was to achieve very similar aromatics- and hydrogen-contents for blend 1 and 2 but at different naphthalene levels. In contrast, the third blend featured similar naphthalene content (as blend 1), but different aromatic content. The measured physical and chemical properties of the fuels evaluated are summarized in Table 1. Due to limited fuel availability, only SAJF1, Ref3 and Ref4 were tested on the engine twice.

Table 2
Test matrix of the ground runs.

Point	N1 [%]	t [min]	Measured values		Estimated[b]
			N1 [%]	Fuel flow [kg/h]	Thrust [%]
1	23[a]	8	–	–	–
2	82	3	78.4 ± 1.9	3197 ± 137	85
3	23[a]	3	–	–	–
4	75	7	74.4 ± 1.2	2737 ± 72	72
5	60	8	59.3 ± 0.7	1589 ± 18	40
6	53	8	53.1 ± 1.2	1270 ± 47	31
7	40	8	39.9 ± 0.5	778 ± 4	18
8	60	8	59.3 ± 1.5	1591 ± 45	40
9	23	8	22.4 ± 0.3	378 ± 5	7

[a] Warm-up or cool-down, not used for analysis (see SI for details).
[b] The engine thrust was estimated on the basis of the measured fuel flow.

The ground test runs were performed with the Airbus A320-232 D-ATRA (Advanced Technology Research Aircraft) of the German Aerospace Center. The ATRA is equipped with two IAE V2527-A5 engines. Measurements were performed on the starboard engine (engine 2) only. At the beginning of the campaign, the engine had been operated for 28,150 flight hours (FH) and 13,060 flight cycles (FC). The test matrix of the ground runs is summarized in Table 2. The different test points were defined on the basis of the same N1 fan speed.

2.1. Sampling

The engine emissions were sampled via a stainless-steel probe that was installed on a blast fence behind the aircraft. No other aircraft were tested while the measurements were being performed. The distance between engine exit and probe inlet was 43 m. The heated transfer line between inlet and measurement container was made of graphitized PTFE. The sample transfer line had a length of 20 m and an inner diameter of 18.5 mm, and was heated to 60 °C. The sample was distributed to the different instruments from a central heated manifold (33 °C) attached to two sampling pumps. The flow through the manifold was controlled via a mass flow controller and set to 137 L/min yielding a Reynolds Number of ~11,500. Various instruments were used to characterize aircraft engine emissions, including the standardized North American Reference System (NARS) for nvPM emission measurements [21,42]. The full setup of instruments is shown in Fig. 1. An intercomparison between the different instruments used for emission measurements and their detailed description are presented elsewhere [38]. Here, the analysis will focus on the effect of the fuel composition on the quantity and characteristics of the nvPM emissions.

2.2. Analytics

Engine exhaust characterization was performed by several different instruments operated by six research groups. A full overview of the instruments is given in Corbin et al. [38]. PM mass and number emissions were measured via three Laser-Induced Incandescence (LII 300, Artium) instruments, two Cavity Attenuated Phase Shift Spectrometers (CAPS PM_{ssa}, Aerodyne Inc.), a Photoacoustic Extinctiometer (PAX, DMT Inc.), two Scanning Mobility Particle Spectrometer (SMPS, TSI Inc.) equipped with a catalytic stripper (CS, Catalytic Instruments) and a thermal denuder (TD, custom-built), a Micro Soot Sensor (MSS, AVL GmbH), a Particle Soot Absorption Photometer (PSAP), a Tricolor Absorption Photometer (TAP, Brechtel Inc.), a DMS 500 Fast Particulate Analyzer

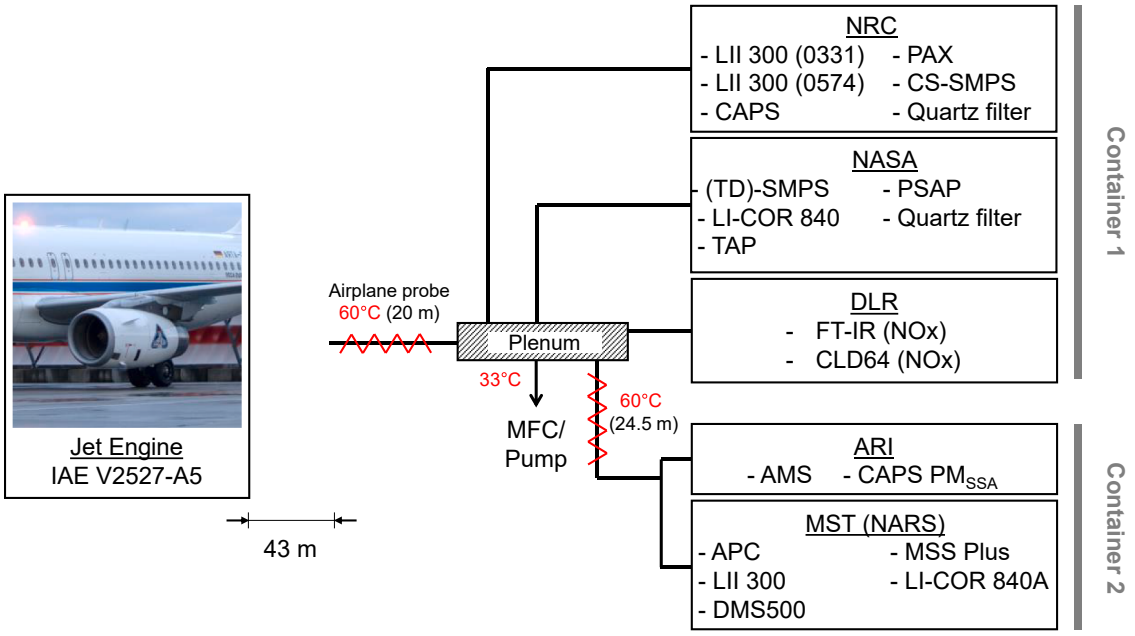

Fig. 1. Sampling setup of the ground measurements in ECLIF2/ND-MAX.

(Cambustion), a AVL Particle Counter (APC) Advanced, and an Aerosol Mass Spectrometer (AMS, Aerodyne Inc.). The instruments included in the North American Reference System (Fig. 1) have been diluted by an ejector diluter with a ratio of 1:4 [38]. Carbon dioxide emissions were monitored with two LI-840(A) CO_2/H_2O non-dispersive Infrared Analyzers (LI-COR) whereas nitrogen oxides (NO_x) were monitored with an MKS MultiGas 2030 FT-IR Continuous Gas Analyzer and a Nitrogen Oxide Analyzer (CLD64, Eco Physics Inc.).

In addition, a SMPS without aerosol treatment, an Engine Exhaust Particle Sizer (EEPS, TSI Inc.) and a Condensation Particle Counter (CPC, TSI Inc.) were operated but the results were not used for the analysis for technical reasons [38]. A Proton-Transfer Reaction Time of Flight Mass Spectrometer (PTR-ToF-MS) with a CHemical Analysis of aeRosol ON-line (CHARON) particle inlet was operated on an additional sampling line to monitor the release of volatiles from the jet engine. The results of this instrument will be reported separately.

2.3. Loss correction

Particle losses in the sampling system were determined experimentally and is described in full detail by Corbin et al. [38]. In short, two SMPS instruments (A: TSI Model 3082 classifier and 3776 CPC, $d_{50} = 3$ nm; B: TSI Model 3082 classifier and 3775 CPC, $d_{50} = 5$ nm) were connected to the inlet and the outlet of the sampling system. The instruments measured particle size in 64 logarithmically-spaced bins over the 11 to 260-nm diameter range. A portable nebulizer and diffusion dryer (Topas GmbH, Model 226) were used to continuously inject ammonium sulfate nanoparticles into a tee connector. Of the two other arms of the tee connector, one was open to atmosphere to intake background make-up air and one was connected to the sampling line. All instruments operated like in the aircraft measurement in order to achieve similar flow conditions in the sampling system. The contribution of entrained ambient air to the resulting aerosol size distribution was negligible. The resulting aerosol size distribution had a count mode diameter of 35 nm and a geometric mean diameter (GMD) of 56 nm and, thus, covered the expected range of the target engine exhaust aerosol. The relative calibrations of the two SMPS systems were established by sampling from the nebulizer using equal line lengths, all other conditions being equal to the loss experiment. The loss correction function was determined on the basis of the ratio of the average particle size distribution at the outlet and the inlet. The size dependent loss correction for the NARS and the other instruments were different due to the additional sample transfer line between container 1 and 2 (Fig. 1).

2.4. Data analysis

Based on an instrument intercomparison study [38], nvPM mass emission indices (nvPM_mass) were derived from the geometric mean of the two CAPS PM_{ssa}, three LII-300 and PAX instruments. nvPM number emission indices (nvPM_num) and particle size distribution were derived from the CS-SMPS system. Measurements from the different instruments were individually loss corrected on the basis of the determined loss function. Based on the carbon dioxide concentration $[CO_2]$ recorded by the NASA LI-840 CO_2/H_2O Analyzer and corrected for the background carbon dioxide concentration $[CO_2]_{BG}$, the emission indices were calculated according to SAE recommended practice [43] from the averaged data.

$$EI_{nvPM\_num}\left[\frac{\#}{kg}\right] = PN\left[\frac{\#}{cm^3}\right]\cdot 10^6 \cdot \frac{R\left[\frac{L\,atm}{K\,mol}\right]\cdot T[K]}{p[atm]\left(M_C\left[\frac{g}{mol}\right] + \alpha \cdot M_H\left[\frac{g}{mol}\right]\right)\cdot([CO_2]-[CO_2]_{BG})} \quad (1)$$

$$EI_{nvPM\_mass}\left[\frac{mg}{kg}\right] = PM\left[\frac{mg}{m^3}\right]\cdot \frac{R\left[\frac{L\,atm}{K\,mol}\right]\cdot T[K]}{p[atm]\left(M_C\left[\frac{g}{mol}\right] + \alpha \cdot M_H\left[\frac{g}{mol}\right]\right)\cdot([CO_2]-[CO_2]_{BG})} \quad (2)$$

The emission indices for particle number (1) and particle mass (2) are calculated from their respective concentrations (PN, PM), the fuel H/C ratio (α), the ideal gas constant (R) and the molar masses for carbon (M_C) and hydrogen (M_H) at standard conditions for temperature (T_m; 273.15 K) and pressure (P_m; 1 atm). The background carbon dioxide concentration has been determined by measuring ambient conditions before each engine start up.

3. Results and discussion

The ground-based tests with the different fuels were performed without any observed adverse impact on the engine. However, the idle

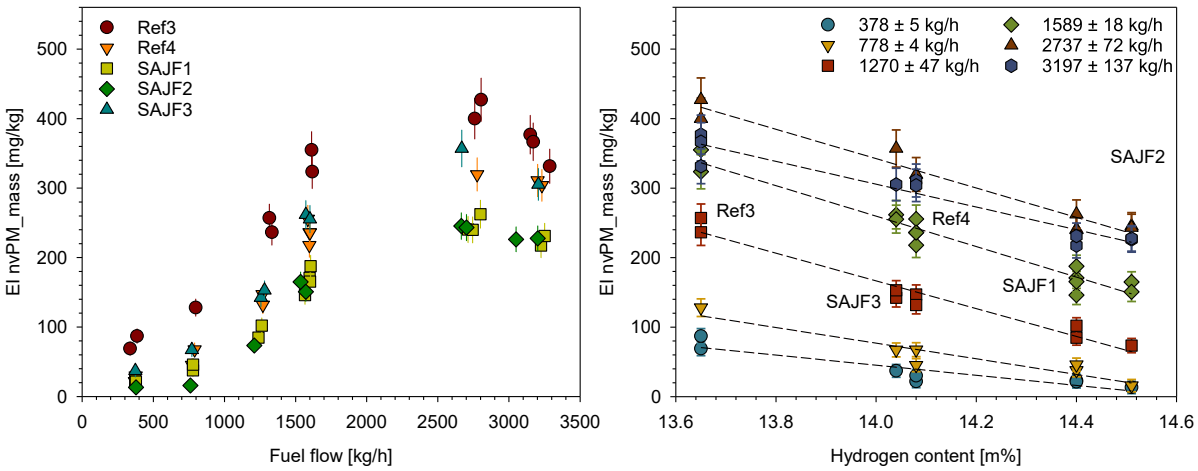

Fig. 2. Non-volatile particulate matter mass emission indices for the different fuels as a function of the measured fuel flow (left) and as a function of the fuel hydrogen content (right). The ordinate axes are the geometric mean of the 7 real-time nvPM sampling instruments discussed in Corbin et al. [38]. The error bars represent the standard deviation of the mean. The dashed lines in the right diagram serve as a guide to the eye.

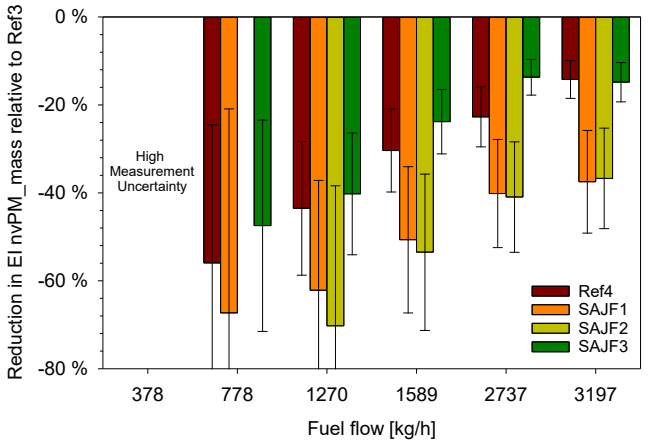

Fig. 3. Reduction in the non-volatile particulate matter mass emission index for the different engine power settings and different fuels using Ref3 as reference.

conditions (23% N1) for operating points 1 and 3 in the test matrix (Table 2) were not used for data analysis due to the changing engine conditions and the variable ambient wind speed and direction. The combustor inlet temperature T3 showed a drift during the warm-up of the engines and within 10 min after finishing the highest power setting (82% N1). The other power settings showed no significant shift in the engine operating parameters.

3.1. Particle mass emission

The emission profile of the IAE V2527-A5 engines shows an increase in nvPM_mass (Fig. 2, left) from fuel flow 378 kg/h (23% N1) to 1589 kg/h (60% N1). Emission measurements within the "keep-out-zone" (61% – 74% N1) were not possible because the engine control prevented stabilized engine operation in this specific fan speed/pressure ratio range. The highest nvPM_mass was observed for 2737 kg/h (75% N1). The nvPM_mass emission profile matches earlier experiments with this engine [23] and shows the expected decrease with increase in fuel hydrogen content (Fig. 2, right) for each power setting. The fuel pairs SAJF3/Ref4 and SAJF1/SAJF2 feature hydrogen contents that are within their respective uncertainty levels of the ASTM D7171 method and thus exhibit comparable nvPM_mass values and similar emission reductions in comparison to Ref3 (Fig. 3). In case of the lowest engine power setting, the calculated reduction showed an elevated uncertainty and was discarded from further analysis. This high uncertainty was caused by the non-ideal wind conditions. The reduction in nvPM_mass tends to decrease with increasing engine power setting. The fuel with the highest hydrogen content, SAJF2, showed a nvPM_mass reduction of (70 ± 23)% at a fuel flow of 1270 kg/h (53% N1) compared to the reference fuel Ref3. At the highest engine power setting, a reduction of (37 ± 11)% was observed for the same fuel. This value is very similar to the reduction observed for SAJF1 of (37 ± 12)%. The second pair of fuels with similar reduction consists of Ref4 ((14 ± 4)%) and SAJF3 of (15 ± 4)%.

SAJF1 and SAJF2 show the same particle mitigation although SAJF2 contains 20 vol% less HEFA-SPK. This effect can be seen even more clearly with SAJF3 since the fuel with similar emission properties (Ref4) is a pure fossil kerosene. The experiment illustrates the necessity to select fossil fuels with suitable properties (e.g. hydrogen content) for blending with available alternative jet fuel components because the emission performance of the blend is directly dependent on that of the base Jet A-1 fuel. More precise, the level of nvPM mass emissions of a blend depends on the amount and type of aromatic compounds in the fossil fuel. Despite the fact that fossil fuels with elevated hydrogen content are available (e.g. Ref4), also the net-release of CO_2 must be considered. Carbon-neutral burning SAF jet fuel components are currently available in much smaller quantities than fossil jet fuel. Therefore, the available amounts have to be used in the most efficient way with regard to possible climate and air quality effects. If the production of high-sooting fossil fuels cannot be avoided, they should be solely applied as SAF blends to reduce overall aviation nvPM emissions especially in areas with high contrail formation potential. With regard to possible climate effects, emitted CO_2 has a persistent long term effect but the mitigation of contrail formation by reduced soot emission is an important aspect in lowering global contrail-cirrus radiative forcing [29].

In this study, the nvPM mass reduction has been estimated relative to the emissions of Ref3. The fuel was selected due to its low hydrogen content and to illustrate the similarities of the blend SAJF3 and the fossil kerosene Ref4. The observed reductions would be smaller if Ref4 had been used instead. Therefore, the reductions should not be generalized – especially not beyond the engine-type used in this experiment.

3.2. Particle number emission and influence of the naphthalene content

The three alternative jet-fuel blends exhibit lower nvPM_num emission indices in the fuel flow range between 778 kg/h (40% N1) and 1270 kg/h (53% N1) compared to the reference kerosene Ref3 (Fig. 4). The difference in particle number emission decreases with increasing

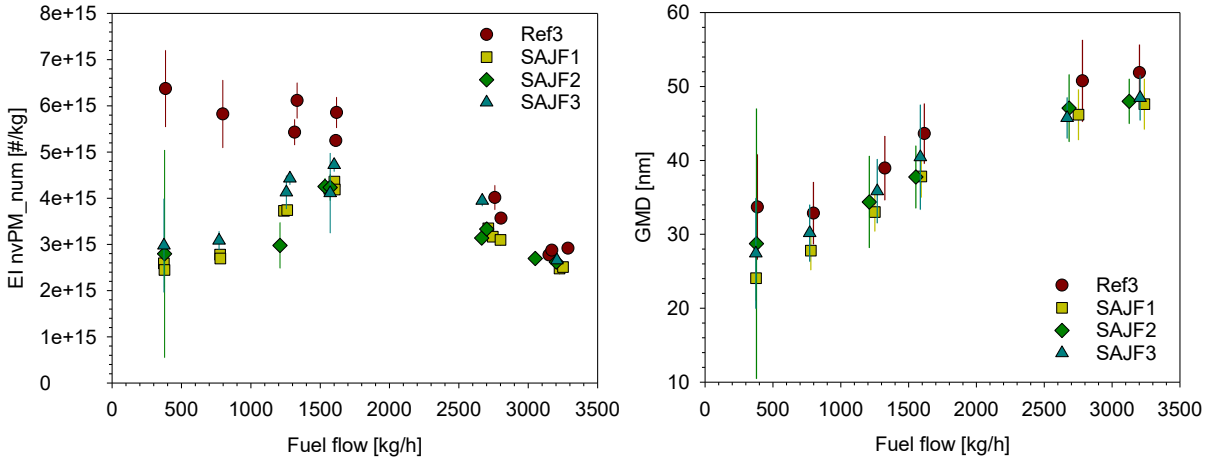

Fig. 4. Non-volatile particulate matter number emission index (left) and geometric mean diameter (right) in dependence of the fuel flow at different power settings from CS-SMPS measurements. The results of Ref4 were excluded due to an instrument error.

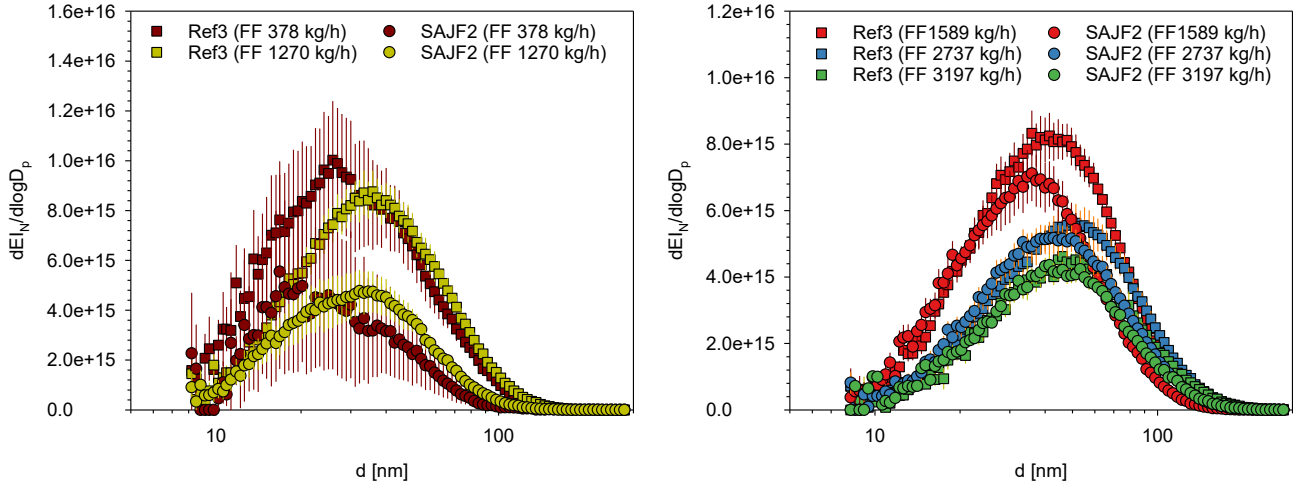

Fig. 5. Non-volatile particle size distribution (CS-SMPS) at low power (left) and high power (right) settings for Ref3 (lowest hydrogen content) and SAJF2 (highest hydrogen content). PSDs for a fuel flow of 778 kg/h had to be excluded due to high error bars in the SAJF2 measurement.

thrust. At the highest power setting of the experiment (85% estimated thrust) the number emission from the different fuels is similar (Fig. 4, left). Regarding the particle size distribution (PSD), the increasing engine power setting is associated with an increase in the geometric mean diameter (GMD) of the particle size distribution. In particular, the GMD of Ref3 is larger than those of the blended fuels (Fig. 4, right). Both factors, higher nvPM_num and larger GMD, account for the differences in nvPM_mass emissions shown in Fig. 2. A comparison between the fuels with the highest and the lowest hydrogen content show the shift in the PSD (Fig. 5) for the different power settings. This observation might be explained by soot formation kinetics as discussed below.

Early studies on the correlation between smoke point and fuel hydrogen content indicated the relevance of the naphthalene content for the prediction of soot emissions [44]. Fundamental combustion studies on individual chemical compounds revealed the different sooting tendency within different molecular classes. A rough comparison may be performed based on the yield sooting index (YSI) of the respective compounds [45,46]. Generally, aliphatic compounds show a lower YSI than aromatic structures. Among the aromatics, higher aromatic structures, such as 1,2-dihydronaphthalene (YSI 100) and anthracene (YSI 195), show significantly higher sooting indices than benzene (YSI 30, by definition). It must be noted that the YSI is a molar based index, and it is not simple to transfer quantitative findings to a kerosene exhibiting a complex mixture of hundreds of different chemicals [47,48] without considerig the full composition. Nevertheless, the described fundamental considerations have been experimentally proven since lab-studies revealed that that the high molecular weight components in fossil kerosene, such as multi-ring structures, have a high impact on the sooting tendency of the fuel [49].

For the fuels applied in this study even experimental investigations of the reaction and soot precursor chemistry obtained in a laminar flow reactor setup [50] under well controlled conditions is available [36]. This study allows for comparison of various soot precursor species formed during the fuel oxidation process under homogeneous premixed conditions. As similar order of sooting propensity was found for typical soot precursor intermediates such as benzene i.e. a reduction compared to Ref4: SAJF1 (-39%) > SAJF2 (-36%) ≫ SAJF3 (–17%) > REF3 (-16%). This is quite comparable to the findings of particle mass reduction at the engine under high load condition (Fig. 3). However, the impact of the naphthalene content was seen to impact the precursor chemistry for larger soot precursors i.e. multi-core aromatics. Considering the fact that regular kerosene may contain up to 20%v/v of aromatics while

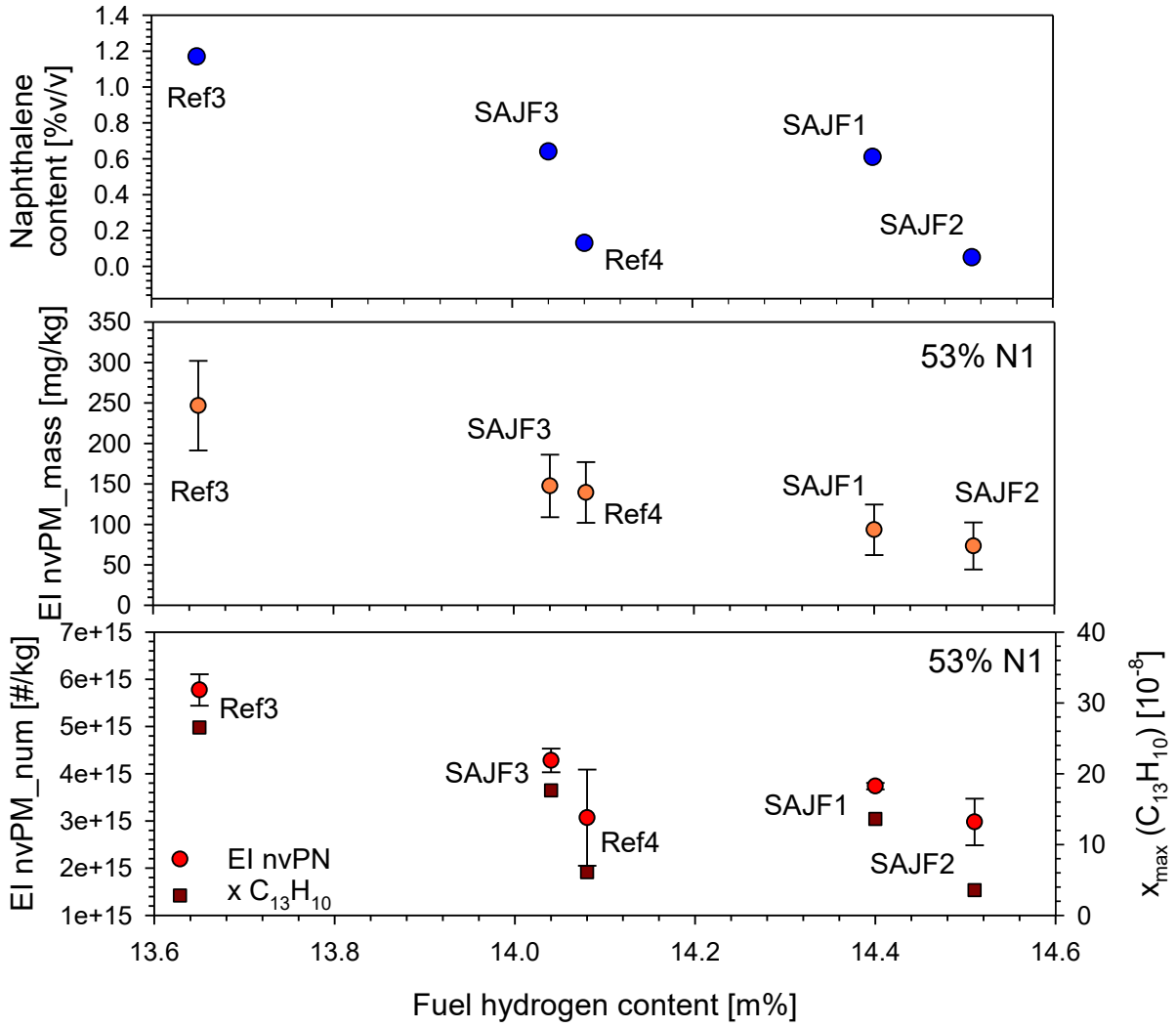

Fig. 6. Comparison between fuel naphthalene content (blue) and the nvPM mass (orange) and nvPM number (red) emission indices measured at intermediate power (1270 kg/h fuel flow, 53 % N1). The uncertainty of the naphthalene content has been estimated on the basis of the reproducibility in ASTM D1840. The number emission diagram contains peak $C_{13}H_{10}$ concentrations found in the flow reactor experiment [36] for comparison.

naphthalenes are allowed to a maximum of 3% it is a complex problem to predict the general sooting tendency of a jet fuel – especially if the fuel composition drastically changes in alternative jet fuels. Based on the low ratio of naphthalenes vs. the sum of aromatic compounds we presume that the naphthalene content should impact the particle number emission to a higher extent than the particle mass emission due to the different number of soot precursors.

In the present study, the fuel mixtures were designed to have no strict correlation between the aromatic content and the naphthalene content. Ref4 and SAJF2 feature a lower amount of naphthalenes than the other fuels of this study considering their aromatic content or hydrogen content (Table 1). Fig. 6 compares the naphthalene content as well as the peak $C_{13}H_{10}$ (fluorene and isomers) concentrations found in the flow reactor experiment [36] of each investigated fuel with the nvPM_mass and nvPM_num emissions at an intermediate power setting with a fuel flow of 1270 kg/h (53% N1). The observed trend of the soot precursor compounds matches the observed particle number emission during the in-field measurements. In addition, nvPM_mass and nvPM_num emission indices have the expected downward trend with increasing H content as also shown in Figs. 2 and 4.

As discussed above, the correlation between hydrogen content and nvPM_mass emission shows no visible deviation for the different naphthalene levels (SAJF3 vs Ref4 and SAJF1 vs SAJF2). In the case of the nvPM_num emission, however, the “steps” in the naphthalene content are mirrored as well as for the soot precursor at the flow reactor. Ref4 and SAJF2 show a lower particle number emission than expected from the emission of Ref3, SAJF1 and SAJF3. At the highest power setting used in this study with a fuel flow of 3197 kg/h (82% N1), a difference between nvPM_num emission from the various fuels can no longer be observed (Fig. 4). Here, the impact of the naphthalene content seems to be no longer relevant. Based on the findings from the soot precursor chemistry one can conclude that the higher amount of multicore combustion intermediates translates to a higher particle number possibly caused by more nucleation possibilities. A similar behavior has been also observed for other jet engines [28,51]. At high power settings the technical parameters of the engine are more important than the chemical composition of the fuel. At high temperature and pressure in the combustion chamber, soot can be formed in the absence of fuel aromatics. Therefore, the reduced soot formation of aliphatic-rich fuels is lower at the highest power settings of a jet engine.

Previous combustor studies at low power settings indicated an increase in emitted particle mass (based on smoke number measurements) when significantly increasing the naphthalene content (4.5%v/v) in a jet fuel [52]. Brem et al. [51] observed an increase of 40% in nvPM_mass and 30% in nvPM_num emissions at low power settings of a high-bypass turbofan engine when changing the naphthalene content from 0.78%v/v

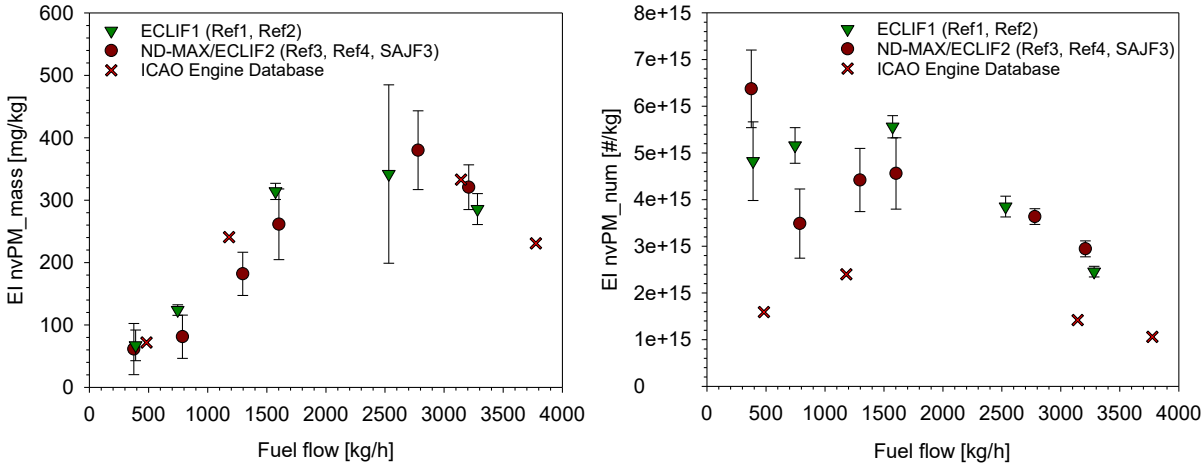

Fig. 7. Comparison of DLR ATRA nvPM_mass (left) and nvPM_num (right) emissions when burning Jet-A reference fuels during ECLIF1 and ND-MAX/ECLIF2. nvPM_mass data are from the NRC 660-nm $CAPS_{SSA}$ (ECLIF2) and the NASA 660-nm $CAPS_{PMEX}$ (ECLIF1), corrected for scattering using the NRC-$CAPS_{SSA}$ values determined as a function of N1. nvPM_num data are from the NRC CS-SMPS (ECLIF2) and the NASA TSI3775 with thermal denuder (ECLIF1). Differences in instrument cut sizes and sampling-system transmission efficiencies may account for some of the differences in values. Certification values are taken from the ICAO database (Table 3).

Table 3
Test rig certification data for the IAE V2527-A5 jet engine [53] based on a kerosene with a hydrogen content of 13.83 %m/m and a naphthalene content 2.38 %v/v.

Condition	Power Setting [% F_{max}]	Fuel flow [kg/h]	nvPM EI_{mass} [mg/kg]	nvPM EI_{num} [#/kg]
Take-Off (T/O)	100	3776.4	230.7	1.06E + 15
Climb-Out (C/O)	85	3142.8	333.0	1.42E + 15
Approach	30	1180.8	240.8	2.40E + 15
Idle	7	482.4	71.9	1.59E + 15

to 1.19%v/v at similar total aromatic content. The authors point out that the precision of the particle mass measurement is reduced at low concentrations. Moore et al. [28] analyzed the effect of 15 different fuels on emissions from a CFM56-2-C1 engine and found that fuel naphthalene content had a significant impact on the nvPM number and mass emissions.

3.3. Comparison to previous findings

PM emissions from the V2527-A5 engines on the DLR ATRA were studied extensively in previous ground and airborne experiments. Within the first ECLIF campaign, 6 different fuels with a hydrogen contents between 14.1%m/m and 14.7%m/m (ASTM D 5291) and naphthalene contents between 0.25%v/v and 1.83%v/v (ASTM D 1840) have been used. The ground measurements showed a nvPM mass emission index of approx. 400 mg/kg for the highest power setting and the fuel with the lowest hydrogen content (Ref1). The results (Fig. 7) are in acceptable agreement to the results of Ref3 in this study which features a similar hydrogen content (Ref1: 13.67%m/m[2]; Ref3: 13.65%m/m). The most recent ICAO Aircraft Engine Emission Databank (2020) now includes information on the nvPM_mass and nvPM_num emissions of currently used jet engines. The fuel specifications are given as well. For the engine type of this study, the results for nvPM_mass are in excellent agreement to test rig certification results (Table 3). The hydrogen content of the certification fuel (13.83%m/m) is also comparable to the hydrogen content of Ref3. Following the trend, the measured nvPM_mass for idle, approach and climb-out for Ref3 are 2% – 8% higher than for the certification fuel. In contrast to the nvPM_mass emission, the release of nvPM_num is lower during the certification measurement – even though the naphthalene content (2.38%v/v) is significantly higher compared to Ref3 (1.17%v/v). Corbin et al. [38] analyzed the uncertainty of the nvPM_num results for this study based on two different volatile particle removers. They showed that the instruments agreed within a factor of 2. Considering this margin of error, the compared nvPM_num emission are within the measurement uncertainty of the instrument. An influence of the aging of the plume cannot be excluded since the certification measurement is performed on the engine exit plane while the in-field measurement was performed at 40 m distance. The aerosol might undergo a shift to a larger particle size distribution due to agglomeration of particles. This would reduce the measured particle number in the field compared to test bed measurements. Since the field results are elevated against the certification measurements instead the particle loss mechanisms seem to be negligible. However, further research on plume evolution is necessary to fully understand the observed deviation in nvPM_num.

The observed emission data at ground level cannot be directly transferred to in-flight conditions due to the different combustor and environmental conditions. Nevertheless, in order to complete the picture, the results at ground level are elevated against the results from flight measurements at ~10 km altitude [9,39,40]. It must be noted that the two fuel blends, SAJF1 and SAJF2, feature only a small difference in fuel hydrogen content (approx. 0.1%m/m). Since the inflight measurements were performed at far-field distances (approx. 7 km) the uncertainties in soot quantification have to be accepted. As a result, the difference in nvPM_num from SAJF1 and SAJF2 is less apparent in the flight measurements but can be observed from the ground measurements at a fuel flow of 1270 kg/h (Fig. 8). Further investigation is necessary to achieve a transferability of the two data sets and allow an estimation of in-flight results based on ground level experiments. The combination of experiments has proven to be useful to explain the different fuel effects over the whole emission profile of the engine and the demonstrate the positive effects of SAF under real-use conditions.

3.4. Emission of nitrogen oxides

The formation and release of nitrogen oxides in jet engine

[2] ASTM D 7171; The values in [16] deviate because the precision of the ASTM D 5291 was not sufficient.

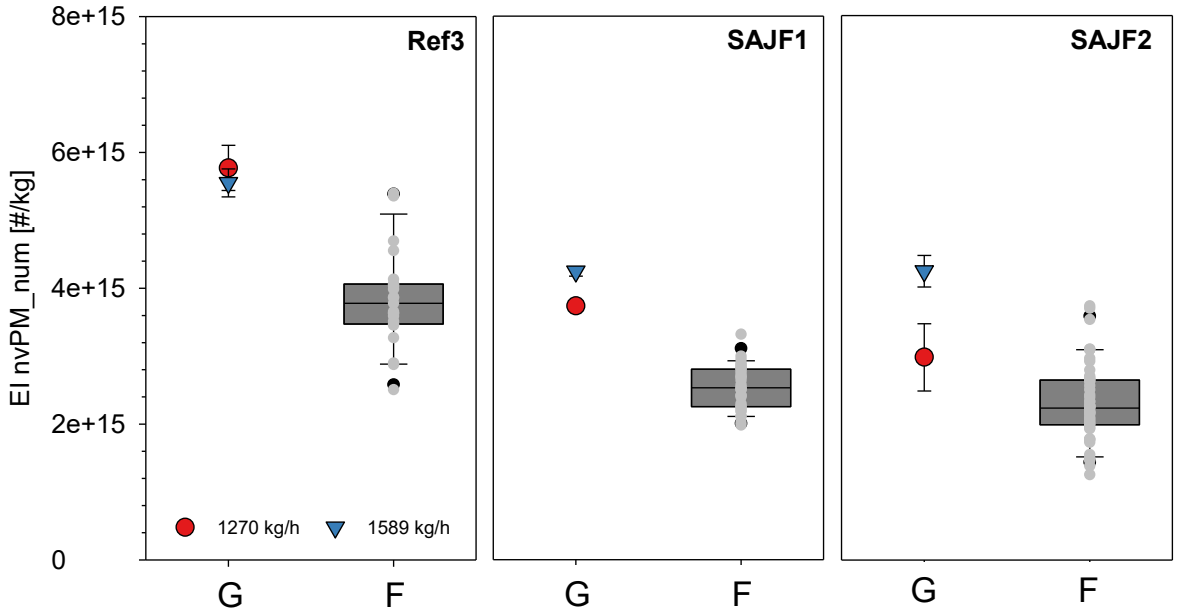

Fig. 8. Comparison between the non-volatile particle number emission indices at ground level (G) and in-flight (F). The inflight data is taken from [9]. The fuel flow of the source engine was 1206 ± 52 kg/h (Ref3), 1132 ± 25 (SAJF1) and 1091 ± 20 kg/h (SAJF2).

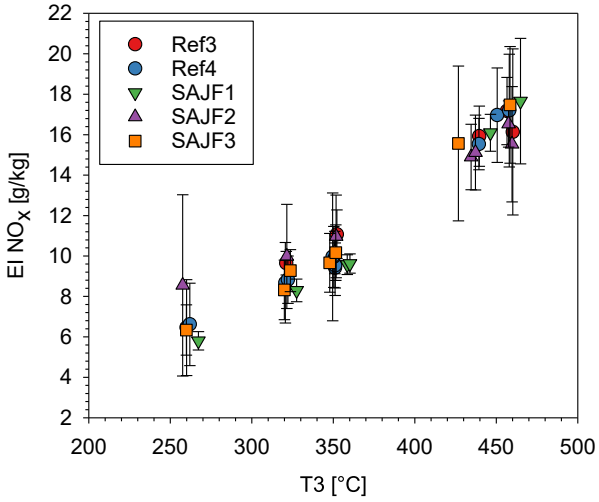

Fig. 9. Emission of nitrogen oxides (NOx) for 5 different fuels in dependence of the combustor inlet temperature T3.

combustors correlates with the combustor inlet temperature T3 [54]. If the physico-chemical properties of a certain fuel (e.g. the heat of combustion) leads to a change in the combustor, an individual shifted correlation between T3 and emission index of NO_x should be visible. In the present case, a significant difference could not be observed within the margin of error (Fig. 9). The ICAO Aircraft Engine Emission Databank (2020) reports a NO_x emission index of 22.3 g/kg for the climb-out condition (85% N1, 0.88 kg/s fuel flow). This condition is in the order of the highest power setting in this study. The observed emission index for nitrogen oxides is slightly lower than expected from this value. This aligns with previous findings for this engine [23]. In summary, the tested fuels did not affect the release of nitrogen oxides in this study. The respective emission indices might be a useful tool to combine the results from ground and in-flight measurements in future analyses.

4. Conclusions

This study experimentally demonstrated that the composition of base Jet A-1 kerosene primarily dictate the nonvolatile particle mass- and number-emission characteristics of SAF blends. The particle mitigation potential of SAF blends tend to decrease with increasing power settings of the engine. While the general trends in particle emission are well reflected by combustion kinetics and soot precursor formation at controlled conditions, the actual soot formation at a full-scale RQL engine is a complex interaction of fuel chemistry, spray formation, turbulent flow field and soot oxidation. In particular, fuel specific influences to the flame structure at different combustor conditions requires further research to gain insights into the fuel effects at high thrust settings.

An additional challenge is that an available alternative jet fuel component needs to be blended with a fossil fuel with suitable properties (e.g. elevated hydrogen content) to optimize particle-reduction benefits, while maintaining full compatibility and performance. The example of Ref4 and SAJF3 demonstrates that the application of alternative jet fuel blends does not necessarily decrease particle emission from the engine. The fuel users need to be enabled to estimate non-CO_2 emission properties of new fuel blends prior to their application to prevent waste of existing alternative jet fuel production capacities without a positive impact on the climate and air quality. This procedure could only be ended by moving to 100% renewable fuel which will require a significant increase in production capacity in the upcoming decades. Regarding the limited quantities of sustainable jet fuel blending components, the development of operable and purposeful fuel design strategies is a vital challenge for future aviation.

Declaration of Competing Interest

The authors declare that they have no known competing financial interests or personal relationships that could have appeared to influence

the work reported in this paper.

Acknowledgements

This work has been funded by the DLR aeronautics program in the framework of the project "Emission and Climate Impact of Alternative Fuels (ECLIF)". The Transport Canada project "TC Aviation — nvPM from renewable and conventional fuels" provided support for the NRC participants and activities as well as additional hours of testing with the ATRA engine. The U.S. Federal Aviation Administration Office of Environment and Energy and the National Aeronautics and Space Administration Aeronautics Research Mission Directorate supported field operations and participation of the U.S researchers in the project. MS&T and ARI received support from the U.S. Federal Aviation Administration (FAA) through the Aviation Sustainability Center (ASCENT) – a U.S. FAA-NASA- U.S. DoD-Transport Canada- U.S. EPA sponsored Center of Excellence for Alternative Jet Fuels and Environment under Grant No. 13-C-AJFE-MST, Amendment 010. A.F. was supported by funds from ARI. The authors are very thankful to the US Airforce 86th Airlift Wing for their hospitality, support and flexible solving of all in-field problems. Special thanks for Dale Bowser (NASA) who provided logistical and communication support and acted as a liaison between the research team and Air Force operations. The authors acknowledge the contribution of the DLR colleagues Jens Heider (Test Pilot), Stefan Seydel (Test Pilot), Peter Baumann (Test Pilot), Georg Mitscher (Test Pilot), Adrian Mueller (Flight Test Engineer), Waldemar Krebs (Flight Test Engineer), Jens Hammer (Technician), Timo Kausche (Technician), Ludger Tegenkamp (FTI Specialist), Stephan Graeber (FTI Specialist) and André Krajewski (Flight Test Project Coordinator) whose support made this successful campaign possible. The authors thank Thomas Bierkandt for his inputs during manuscript revision.

Appendix A. Supplementary data

Supplementary data to this article can be found online at https://doi.org/10.1016/j.fuel.2022.124764.

References

[1] International Energy Agency (IEA). IEA Oil Information: Overview (https://www.iea.org/reports/oil-information-overview). 2021.
[2] U.S. Energy Information Administration (EIA). Flight data confirm changes in overall U.S. jet fuel consumption estimates. This Week in Petroleum 2020;26. August 2020.
[3] Reifenberg SF, Martin A, Kohl M, Hamryszczak Z, Tadic I, Röder L, et al. Impact of reduced emissions on direct and indirect aerosol radiative forcing during COVID–19 lockdown in Europe. Atmos Chem Phys Discuss 2021;2021:1–23. https://doi.org/10.5194/acp-2021-1005.
[4] Voigt C, Lelieveld J, Schlager H, Schneider J, Curtius J, Meerkötter R, et al. Cleaner skies during the COVID-19 lockdown. Bull Am Meteorol Soc 2022. https://doi.org/10.1175/bams-d-21-0012.1.
[5] Schumann U, Bugliaro L, Dornbrack A, Baumann R, Voigt C. Aviation Contrail Cirrus and Radiative Forcing Over Europe During 6 Months of COVID-19. Geophys Res Lett 2021;48(8). https://doi.org/10.1029/2021gl092771.
[6] Schumann U, Poll I, Teoh R, Koelle R, Spinielli E, Molloy J, et al. Air traffic and contrail changes over Europe during COVID-19: a model study. Atmos Chem Phys 2021;21(10):7429–50. https://doi.org/10.5194/acp-21-7429-202110.5194/acp-21-7429-2021-supplement.
[7] IATA. Developing Sustainable Aviation Fuel (SAF) (https://www.iata.org/en/programs/environment/sustainable-aviation-fuels). 2021.
[8] Moore RH, Thornhill KL, Weinzierl B, Sauer D, D'Ascoli E, Kim J, et al. Biofuel blending reduces particle emissions from aircraft engines at cruise conditions. Nature 2017;543(7645):411–5. https://doi.org/10.1038/nature21420.
[9] Voigt C, Kleine J, Sauer D, Moore RH, Bräuer T, Le Clercq P, et al. Cleaner burning aviation fuels can reduce contrail cloudiness. Communications Earth & Environment 2021;2(1). https://doi.org/10.1038/s43247-021-00174-y.
[10] Hall C, Rauch B, Bauder U, Le Clercq P, Aigner M. Predictive Capability Assessment of Probabilistic Machine Learning Models for Density Prediction of Conventional and Synthetic Jet Fuels. Energy Fuels 2021;35(3):2520–30. https://doi.org/10.1021/acs.energyfuels.0c0377910.1021/acs.energyfuels.0c03779.s001.
[11] Corporan E, Edwards T, Shafer L, DeWitt MJ, Klingshirn C, Zabarnick S, et al. Chemical, Thermal Stability, Seal Swell, and Emissions Studies of Alternative Jet Fuels. Energy Fuels 2011;25(3):955–66. https://doi.org/10.1021/ef101520v.
[12] Lobo P, Hagen DE, Whitefield PD. Comparison of PM Emissions from a Commercial Jet Engine Burning Conventional, Biomass, and Fischer-Tropsch Fuels. Environ Sci Technol 2011;45(24):10744–9. https://doi.org/10.1021/es201902e.
[13] Beyersdorf AJ, Timko MT, Ziemba LD, Bulzan D, Corporan E, Herndon SC, et al. Reductions in aircraft particulate emissions due to the use of Fischer-Tropsch fuels. Atmos Chem Phys 2014;14(1):11–23. https://doi.org/10.5194/acp-14-11-201410.5194/acp-14-11-2014-supplement.
[14] Schripp T, Herrmann F, Oßwald P, Köhler M, Zschocke A, Weigelt D, et al. Particle emissions of two unblended alternative jet fuels in a full scale jet engine. Fuel 2019;256:115903. https://doi.org/10.1016/j.fuel.2019.115903.
[15] Boeing. Boeing Commits to Deliver Commercial Airplanes Ready to Fly on 100% Sustainable Fuels (https://boeing.mediaroom.com/2021-01-22-Boeing-Commits-to-Deliver-Commercial-Airplanes-Ready-to-Fly-on-100-Sustainable-Fuels) 22.01.2021.
[16] United. United to Become First in Aviation History to Fly Aircraft Full of Passengers Using 100% Sustainable Fuel (https://www.united.com/en/us/newsroom/announcements/united-to-become-first-in-aviation-history-to-fly-aircraft-full-of-passengers-using-100-sustainable-fuel). 2021.
[17] Petzold A, Busen R, Schröder FP, Baumann R, Kuhn M, Ström J, et al. Near-field measurements on contrail properties from fuels with different sulfur content. J Geophys Res-Atmos 1997;102(D25):29867–80. https://doi.org/10.1029/97JD02209.
[18] Yu FQ, Turco RP. Contrail formation and impacts on aerosol properties in aircraft plumes: Effects of fuel sulfur content. Geophys Res Lett 1998;25(3):313–6. https://doi.org/10.1029/97gl03695.
[19] Jeßberger P, Voigt C, Schumann U, Sölch I, Schlager H, Kaufmann S, et al. Aircraft type influence on contrail properties. Atmos Chem Phys 2013;13(23):11965–84. https://doi.org/10.5194/acp-13-11965-2013.
[20] Kärcher B, Yu F. Role of aircraft soot emissions in contrail formation. Geophys Res Lett 2009;36:5. https://doi.org/10.1029/2008gl036649.
[21] Lobo P, Condevaux J, Yu Z, Kuhlmann J, Hagen DE, Miake-Lye RC, et al. Demonstration of a Regulatory Method for Aircraft Engine Nonvolatile PM Emissions Measurements with Conventional and Isoparaffinic Kerosene fuels. Energy Fuels 2016;30(9):7770–7. https://doi.org/10.1021/acs.energyfuels.6b01581.
[22] Christie S, Lobo P, Lee D, Raper D. Gas Turbine Engine Nonvolatile Particulate Matter Mass Emissions: Correlation with Smoke Number for Conventional and Alternative Fuel Blends. Environ Sci Technol 2017;51(2):988–96. https://doi.org/10.1021/acs.est.6b03766.
[23] Schripp T, Anderson B, Crosbie EC, Moore RH, Herrmann F, Oßwald P, et al. Impact of Alternative Jet Fuels on Engine Exhaust Composition During the 2015 ECLIF Ground-Based Measurements Campaign. Environ Sci Technol 2018;52(8):4969–78. https://doi.org/10.1021/acs.est.7b0624410.1021/acs.est.7b06244.s001.
[24] Kinsey JS, Squier W, Timko M, Dong Y, Logan R. Characterization of the Fine Particle Emissions from the Use of Two Fischer-Tropsch Fuels in a CFM56-2C1 Commercial Aircraft Engine. Energy Fuels 2019;33(9):8821–34. https://doi.org/10.1021/acs.energyfuels.9b0078010.1021/acs.energyfuels.9b00780.s001.
[25] Elser M, Brem BT, Durdina L, Schönenberger D, Siegerist F, Fischer A, et al. Chemical composition and radiative properties of nascent particulate matter emitted by an aircraft turbofan burning conventional and alternative fuels. Atmos Chem Phys 2019;19(10):6809–20. https://doi.org/10.5194/acp-19-6809-201910.5194/acp-19-6809-2019-supplement.
[26] Durdina L, Brem BT, Elser M, Schönenberger D, Siegerist F, Anet JG. Reduction of Nonvolatile Particulate Matter Emissions of a Commercial Turbofan Engine at the Ground Level from the Use of a Sustainable Aviation Fuel Blend. Environ Sci Technol 2021;55(21):14576–85. https://doi.org/10.1021/acs.est.1c0474410.1021/acs.est.1c04744.s00110.1021/acs.est.1c04744.s002.
[27] Schripp T, Grein T, Zinsmeister J, Oßwald P, Köhler M, Müller-Langer F, et al. Technical Application of a Ternary Alternative Jet Fuel Blend – Chemical Characterization and Impact on Jet Engine Particle Emission. Fuel 2021;288:119606. https://doi.org/10.1016/j.fuel.2020.119606.
[28] Moore RH, Shook M, Beyersdorf A, Corr C, Herndon S, Knighton WB, et al. Influence of Jet Fuel Composition on Aircraft Engine Emissions: A Synthesis of Aerosol Emissions Data from the NASA APEX, AAFEX, and ACCESS Missions. Energy Fuels 2015;29(4):2591–600. https://doi.org/10.1021/ef502618w.
[29] Burkhardt U, Bock L, Bier A. Mitigating the contrail cirrus climate impact by reducing aircraft soot number emissions. Clim Atmos Sci 2018;1:7. https://doi.org/10.1038/s41612-018-0046-4.
[30] Kleine J, Voigt C, Sauer D, Schlager H, Scheibe M, Jurkat-Witschas T, et al. In Situ Observations of Ice Particle Losses in a Young Persistent Contrail. Geophys Res Lett 2018;45(24). https://doi.org/10.1029/2018GL079390.
[31] Lobo P, Christie S, Khandelwal B, Blakey SG, Raper DW. Evaluation of Non-volatile Particulate Matter Emission Characteristics of an Aircraft Auxiliary Power Unit with Varying Alternative Jet Fuel Blend Ratios. Energy Fuels 2015;29(11):7705–11. https://doi.org/10.1021/acs.energyfuels.5b01758.
[32] Liati A, Schreiber D, Alpert PA, Liao Y, Brem BT, Arroyo PC, et al. Aircraft soot from conventional fuels and biofuels during ground idle and climb-out conditions: Electron microscopy and X-ray micro-spectroscopy. Environ Pollut 2019;247:658–67. https://doi.org/10.1016/j.envpol.2019.01.078.
[33] Vander Wal RL, Bryg VM, Huang CH. Aircraft engine particulate matter: Macro-micro- and nanostructure by HRTEM and chemistry by XPS. Combust Flame 2014;161(2):602–11. https://doi.org/10.1016/j.combustflame.2013.09.003.
[34] Kathrotia T, Oßwald P, Naumann C, Richter S, Köhler M. Combustion kinetics of alternative jet fuels, Part-II: Reaction model for fuel surrogate. Fuel 2021;302:120736. https://doi.org/10.1016/j.fuel.2021.120736.

[35] Kathrotia T, Oßwald P, Zinsmeister J, Methling T, Köhler M. Combustion kinetics of alternative jet fuels, Part-III: Fuel modeling and surrogate strategy. Fuel 2021;302:120737. https://doi.org/10.1016/j.fuel.2021.120737.
[36] Oßwald P, Zinsmeister J, Kathrotia T, Alves-Fortunato M, Burger V, van der Westhuizen R, et al. Combustion kinetics of alternative jet fuels, Part-I: Experimental flow reactor study. Fuel 2021;302:120735. https://doi.org/10.1016/j.fuel.2021.120735.
[37] Pelucchi M, Oßwald P, Pejpichestakul W, Frassoldati A, Mehl M. On the combustion and sooting behavior of standard and hydro-treated jet fuels: An experimental and modeling study on the compositional effects. Proc Combust Inst 2021;38(1):523–32. https://doi.org/10.1016/j.proci.2020.06.353.
[38] Corbin JC, Schripp T, Anderson B, Smallwood G, LeClercq P, Crosbie E, et al. Aircraft-engine particulate matter emissions from conventional and sustainable aviation fuel combustion: comparison of measurement techniques for mass, number, and size. Atmos Meas Tech 2022;15(10):3223–42. https://doi.org/10.5194/amt-15-3223-2022.
[39] Bräuer T, Voigt C, Sauer D, Kaufmann S, Hahn V, Scheibe M, et al. Airborne Measurements of Contrail Ice Properties-Dependence on Temperature and Humidity. Geophys Res Lett 2021;48(8). https://doi.org/10.1029/2020GL092166.
[40] Bräuer T, Voigt C, Sauer D, Kaufmann S, Hahn V, Scheibe M, et al. Reduced ice number concentrations in contrails from low-aromatic biofuel blends. Atmos Chem Phys 2021;21(22):16817–26. https://doi.org/10.5194/acp-21-16817-2021.
[41] ASTM D1655-20d. Standard Specification for Aviation Turbine Fuels. 2020.
[42] Lobo P, Durdina L, Brem BT, Crayford AP, Johnson MP, Smallwood GJ, et al. Comparison of standardized sampling and measurement reference systems for aircraft engine non-volatile particulate matter emissions. J Aerosol Sci 2020;145:105557. https://doi.org/10.1016/j.jaerosci.2020.105557.
[43] SAE international. erospace Recommended Practice (ARP) 6320 – Procedure for the Continuous Sampling and Measurement of Non-Volatile Particulate Matter Emissions from Aircraft Turbine Engines. Warrendale, PA. 2018.
[44] Chin JS, Lefebvre AH. Influence of fuel chemical-properties on soot emissions from gas-turbine combustors. Combust Sci Technol 1990;73(1–3):479–86. https://doi.org/10.1080/00102209008951664.
[45] McEnally CS, Pfefferle LD. Improved sooting tendency measurements for aromatic hydrocarbons and their implications for naphthalene formation pathways. Combust Flame 2007;148(4):210–22. https://doi.org/10.1016/j.combustflame.2006.11.003.
[46] McEnally CS, Pfefferle LD. Sooting tendencies of nonvolatile aromatic hydrocarbons. Proc Combust Inst 2009;32(1):673–9. https://doi.org/10.1016/j.proci.2008.06.197.
[47] Spicer CW, Holdren MW, Smith DL, Hughes DP, Smith MD. Chemical-composition of exhaust from aircraft turbine-engines. J Eng Gas Turbines Power-Trans ASME 1992;114(1):111–7. https://doi.org/10.1115/1.2906292.
[48] Wang H, Xu R, Wang K, Bowman CT, Hanson RK, Davidson DF, et al. A physics-based approach to modeling real-fuel combustion chemistry – I. Evidence from experiments, and thermodynamic, chemical kinetic and statistical considerations. Combust Flame 2018;193:502–19. https://doi.org/10.1016/j.combustflame.2018.03.019.
[49] Saggese C, Singh AV, Xue X, Chu C, Kholghy MR, Zhang T, et al. The distillation curve and sooting propensity of a typical jet fuel. Fuel 2019;235:350–62. https://doi.org/10.1016/j.fuel.2018.07.099.
[50] Oßwald P, Köhler M. An atmospheric pressure high-temperature laminar flow reactor for investigation of combustion and related gas phase reaction systems. Rev Sci Instrum 2015;86(10):105–9. https://doi.org/10.1063/1.4932608.
[51] Brem BT, Durdina L, Siegerist F, Beyerle P, Bruderer K, Rindlisbacher T, et al. Effects of Fuel Aromatic Content on Nonvolatile Particulate Emissions of an In-Production Aircraft Gas Turbine. Environ Sci Technol 2015;49(22):13149–57. https://doi.org/10.1021/acs.est.5b04167.
[52] Bowden TT, Carrier DM, Courtenay LW. Correlations of fuel performance in a full-scale commercial combustor and 2 model combustors. J Eng Gas Turbines Power-Trans ASME 1988;110(4):686–9. https://doi.org/10.1115/1.3240192.
[53] EASA. ICAO Aircraft Engine Emissions Databank (https://www.easa.europa.eu, 23.12.2020). 2020.
[54] Chandrasekaran N, Guha A. Study of Prediction Methods for NOx Emission from Turbofan Engines. J Propul Power 2012;28(1):170–80. https://doi.org/10.2514/1.B34245.